COMSOL CONFERENCE 2023 MUNICH

Numerical Simulation of Laser Lithotripsy

A. MENAESSE[1], V. BRUYERE[2], P. NAMY[2], V. GATINEAU[1], G. SPIEZIA[1]
1. EMS, Ch. de la Vuarpillière, 31CH-1260 NYON, SWITZERLAND
2. SIMTEC, 5 rue Felix Poulat, GRENOBLE, FRANCE

Abstract
The use of lasers to fragment and remove kidney stones (Laser Lithotripsy) has become increasingly popular in surgical procedure due to its high success rate and minimal complications. However, the precise mechanisms behind the stone fragmentation process are not yet fully understood. The objective of this work is to develop a numerical model to determine the dimensions of the crater (depth, width) generated by the application of a laser on a study material (Begostone). Given the complexity of the mechanisms involved, a simplified approach is proposed to treat the formation of the crater from a threshold temperature and by using a deformed geometry. The numerical results obtained are then compared to in-vitro experimental results for different fiber widths and several energies to validate this numerical approach.

Keywords: Laser Heating, Heat Transfer, Deformed Geometry

Introduction

During a laser lithotripsy procedure, the laser beam is delivered directly to the kidney stone through an optical fiber inserted inside an endoscope. The stone is then destroyed through a combination of thermal, mechanical and chemical processes.
Performing in vitro experiments allows a precise control of the input parameters (such as the laser beam sequence, the distance between the fiber and the stone…) and a quantitative measurement of the impact on the stone. Nevertheless, the precise material properties and the quantitative contribution of each type of laser-material interaction remain unknown and difficult to measure experimentally.
Therefore, modeling is a convincing approach to provide relevant elements for study and reflection in order to further master the process. A thermal numerical model with material ablation is developed and presented in this work. Its aim is to predict the depth, radius and volume of the crater formed by the laser impact depending on the operating conditions (laser power, laser beam radius, type of impacted material…). After parametric studies, a validation with experimental elements is carried out to guarantee the validity of the chosen approach on a various range of operating conditions.

Modeling and Governing Equations

Each "physics" implemented in COMSOL Multiphysics® is detailed with the different assumptions used in this work.

Heat Transfer
The temperature evolution is predicted by solving the time dependent energy equation, through its conduction form:

$$\rho C_p \frac{\partial T}{\partial t} + \nabla \cdot [-k\nabla T] = 0 \qquad \textit{Eq. 1}$$

where T is the temperature, ρ the density, k the thermal conductivity and C_p the heat capacity of the material.

Laser Source
Before impacting the material under study, the laser wave passes through an aqueous medium. It then interacts with the solid material, leading to its vaporisation and local dislocation. During the laser-matter interaction, complex phenomena take place [1], dissipating energy and requiring a specific study for their precise description. They will be simplified in this approach through a material absorption coefficient.

The energy deposition is assumed to be Gaussian and is modelled by a boundary heat flux. The thermal inward heat flux, q_{in}, is formulated as:

$$q_{in} = P_{laser}(t)\frac{A_0}{\pi\left(\frac{d}{2}\right)^2} e^{-\frac{r^2}{\left(\frac{d}{2}\right)^2}} e^{\frac{z}{\delta_z}} \qquad \textit{Eq. 2}$$

where $P_{laser}(t)$ is the peak laser power function of time, A_0, the surface absorptivity, d, the beam waist and δ_z an attenuation coefficient.

For large laser beam radius ($d > 550\mu m$), the spatial distribution is adapted due to a modification of the Gaussian shape for those high fibre radii. A correction factor of $d = 0.7 * d_{true}$ is used.

The peak laser power $P_{laser}(t)$ is computed from the average power P_{ave} and the power time distribution

$f_{deposition}(t)$ is the power time distribution (unit-less quantity), represented by a rectangle function:

$$f_{deposition}(t) = \begin{cases} 1 \; if \; t \in [0, \tau_{laser}] \\ 0 \; if \; t > \tau_{laser} \end{cases} \qquad Eq.\ 3$$

where the pulse duration is referred to as τ_{laser}.

As the average power is the average of the laser power over a period, $P_{laser}(t)$ should satisfy the following equation:

$$P_{ave} \cdot \frac{1}{f} = \int_{t\in[0;1/f]} P_{laser}(t) \cdot f_{deposition}(t)dt \qquad Eq.\ 4$$

where f is the frequency of the laser pulses.

A spatial representation of the laser power density is given in Figure 1.

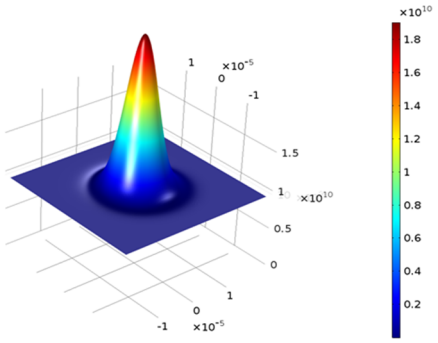

Figure 1. Power density distribution in $[W/m^2]$

Ablation Modeling

In this approach, only the solid phase is modelled meaning the fluid around the component and the vaporised matter are not geometrically considered. To compute the shape of the solid component after one laser impact and obtain the resulting crater depth and volume, the assumption that the solid material surface temperature does not significantly exceed a certain threshold temperature, T_{vap}, is made. In the model, this assumption is expressed by the use of the convective flux boundary condition defined as:

$$\Phi_{vap} = h(T - T_{vap}) \qquad Eq.\ 5$$

where Φ_{vap} is the vaporised flux, h is a numerical parameter and T_{vap} is the vaporization temperature.

At the solid/gas interface, the energy equilibrium is assumed and is expressed as:

$$\rho L_v \boldsymbol{u_{vap}} \cdot \boldsymbol{n} = \Phi_{vap} \cdot \boldsymbol{n} \qquad Eq.\ 6$$

where L_v is the latent heat of vaporization, $\boldsymbol{u_{vap}}$, the velocity of the matter leaving the interface and $\boldsymbol{n}$ the normal vector of the solid front.

The surface is considered free to move to accommodate the change in geometry due to the matter loss. The Deformed Geometry interface is used by setting the normal mesh velocity v_n at the solid gas interface to:

$$v_n = \frac{\Phi_{vap}}{\rho L_v} \qquad Eq.\ 7$$

Numerical Aspects

The Deformed Geometry and Heat Transfer in Fluids interfaces are solved together in a fully coupled way. To obtain more precise results and robust convergence, the normal mesh velocity is prescribed using weak constraints and quadratic Lagrange discretization is used for the temperature.

The mesh is refined near the solid/gas interface where the temperature gradient is important and the surface deformation higher. A representation is given in Figure 2 showing the initial mesh on the left, and the final mesh on the right after one impact. A hyper-elastic smoothing method is used to control the deformation of the mesh. The elements are rigid at the top, allowing them to be moved without too much deformation. At the bottom, the elements are larger and deform more significantly, away from temperature variations.

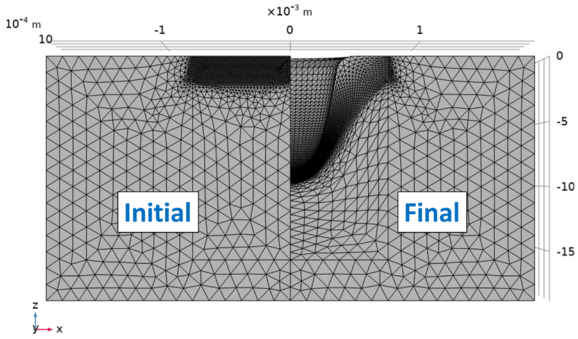

Figure 2 - Initial mesh on the left, Deformed mesh on the right

The computational time for one laser impact and with 128Go and 2.4Ghz Intel® processor is around 2 minutes. The calculation time is optimized to handle a large number of configurations, and the model can also be deployed, via an application, on less powerful computers.

Results

After numerical validation, the model is used to predict the dimensions of a crater after one impact in a reference configuration.

Temperature at the center point and crater depth evolutions are plotted in Figure 3 as a function of time. The temperature very quickly reaches the

vaporization threshold temperature (in blue, Figure 3), set for this material at $T = 200°C$. Due to strong vaporization, the matter is ejected, and a crater is formed. The penetration depth (defined as the opposite of the crater depth and plotted in green, Figure 3) is decreasing to reach a stationary value at the end of the laser pulse ($t = 8ms$). The cooling phase then begins, and the temperature of the material tends towards ambient temperature.

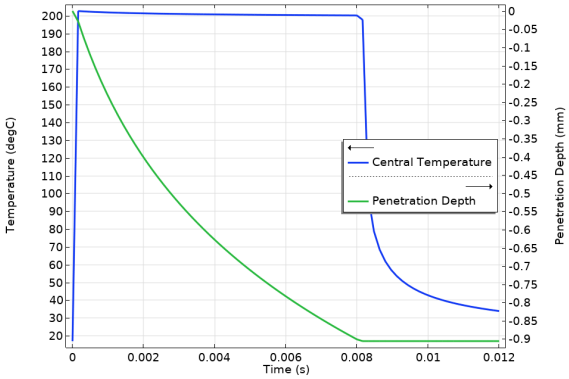

Figure 3. Temperature at the center (left axis) and Crater depth (right axis) as a function of time

A 3D representation of the crater obtained at $t = 8ms$ is shown in Figure 4. For this configuration a depth of 900 µm and a crater volume of 0.23 mm^3 are obtained. These values are the essential output values for calibrating the power to be injected into the lithotripsy process.

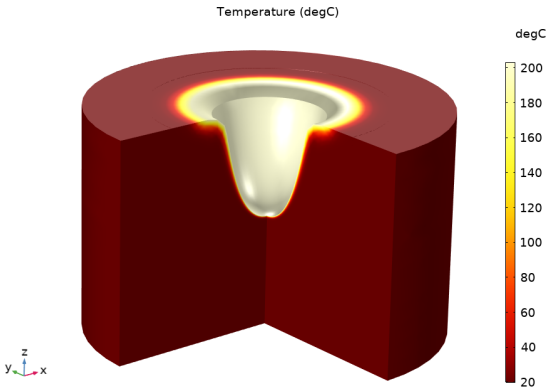

Figure 4. Temperature distribution and resulting crater geometry at $t = 8ms$

Parametric studies

The influence of the chosen threshold temperature T_{vap} is studied here. Its value is indeed not well known in the literature, and its effect on penetration and volume is currently being investigated. The results obtained for three different vaporization temperature values are plotted in Figure 5. No significant influence was observed for this parameter limiting its impact on results.

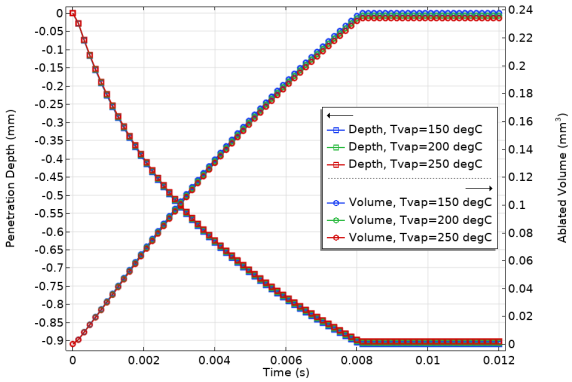

Figure 5. Influence of the threshold temperature on the crated depth (left axis) and on the ablated volume (right axis) as a function of time

An important parameter is the latent heat of vaporization. Indeed, as expressed in Eq. 7, the rate at which the crater deepens is directly linked to the value of the evaporation flux and the latent heat of the material. A parametric study is performed for three values of this parameter around the reference value. Results are shown in Figure 6 for the penetration depth and volume.

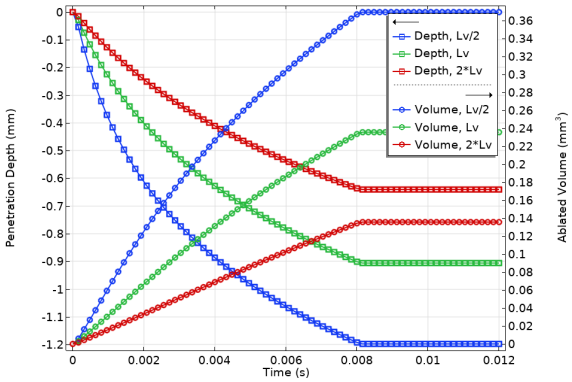

Figure 6. Influence of the latent heat of vaporization on the crated depth (left axis) and on the ablated volume (right axis) as a function of time

With a higher latent heat ($2 * Lv$), the amount of energy required to vaporize the material is higher, and the volume of material vaporized is lower around -40% (red circle, Figure 6) compared to the reference value (green circle, Figure 6). Same tendencies are obtained for the depth with variation of $\pm$ 30% with a factor two on the latent heat.

Comparison with experimental data

In order to validate more quantitatively the model, different operating conditions are then simulated and compared with experimental results. Experimental results have been obtained for six different laser pulse radii and six pulse energies for each leading to a total of thirty-six configurations. Final crater volumes are plotted in Figure 7 with experimental data in red and numerical predictions in blue. It can be observed that numerical curves are very close for each laser pulse relaying the fact that the ablated volume is directly linked to the applied pulse energy and not a direct function of the laser beam radius.

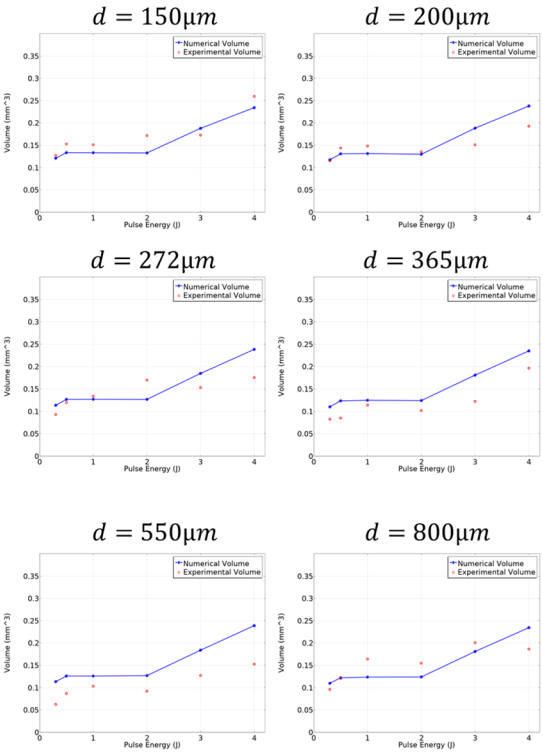

Figure 7. Crater volumes for different laser beam radius and pulse energies – Experimental results (red markers), numerical results (blue lines)

The same work is performed for the final crater depth prediction evolutions in Figure 8. Depending on the laser beam radius, the results are very different. Indeed, the radius of the crater is greater for larger beam radii. For an equivalent ablated volume, penetration is therefore lower for larger beam radii.

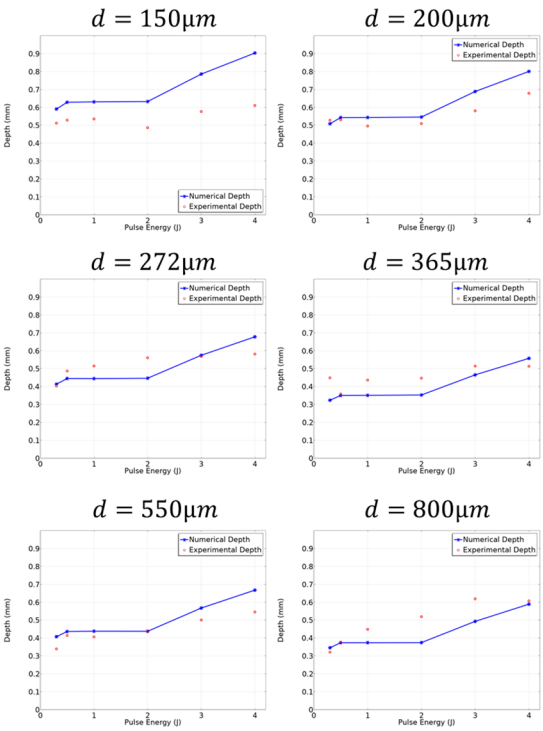

Figure 8. Crater depths for different laser beam radius and pulse energies – Experimental results (red markers), numerical results (blue lines)

Development of an Application

To take advantage of the possibility offered by COMSOL Multiphysics® to generate a simplified and synthetic interface, an application was created. This application can be used to define all the laser and laser-matter interaction parameters presented here, as well as a user-defined temporal power profile. The simulation then takes just a few minutes to run on a standard PC, giving the ablated volume, depth, and radius of the final crater.

A representation of one of the interface tabs is provided in Figure 9.

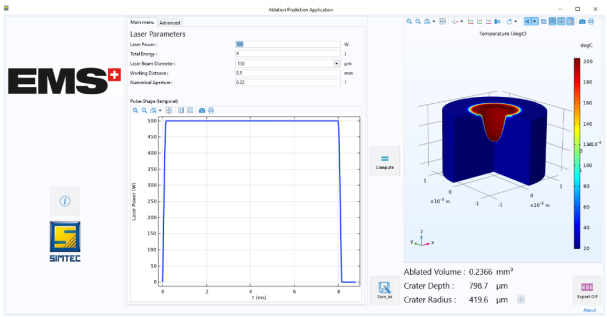

Figure 9. Ablation Prediction Application

Conclusions

A thermal model with material ablation has been developed to improve control of the laser lithotripsy process. The model was used to predict the dimensions of the crater formed during very local heating. In order to compare the model with experimental results, several parameters were studied, such as the size of the laser beam and the energy deposited. The model was able to provide very accurate trends, given the experimental dispersion associated with the complexity of the subject, for the volume and penetration depths.

In order to improve its predictivity and apply it to other material types, further developments are required. In particular, depending on the operating conditions, laser-matter interaction could play a more important role in crater geometry prediction.

References

[1] V. LEROY, "Bulles d'air dans l'eau : couplage d'oscillateurs harmoniques et excitation paramétrique," Thèse, Université Paris 7, 2004.